THE JOURNAL OF BIOLOGICAL CHEMISTRY VOL. 283, NO. 22, pp. 15250–15257, May 30, 2008

γ-Aminobutyric Acid (GABA) and Pentobarbital Induce Different Conformational Rearrangements in the $GABA_A$ Receptor α_1 and β_2 Pre-M1 Regions*

Received for publication, October 18, 2007, and in revised form, March 12, 2008 Published, JBC Papers in Press, April 3, 2008, DOI 10.1074/jbc.M708638200

Jose Mercado[‡] **and Cynthia Czajkowski**[‡§1]

From the [‡]*Department of Physiology and the* [§]*Neuroscience Training Program, University of Wisconsin-Madison , Madison, Wisconsin 53706*

γ-Aminobutyric acid (GABA) binding to $GABA_A$ receptors ($GABA_A$Rs) triggers conformational movements in the α_1 and β_2 pre-M1 regions that are associated with channel gating. At high concentrations, the barbiturate pentobarbital opens $GABA_A$R channels with similar conductances as GABA, suggesting that their open state structures are alike. Little, however, is known about the structural rearrangements induced by barbiturates. Here, we examined whether pentobarbital activation triggers movements in the $GABA_A$R pre-M1 regions. $\alpha_1\beta_2$ $GABA_A$Rs containing cysteine substitutions in the pre-M1 α_1 (K219C, K221C) and β_2 (K213C, K215C) subunits were expressed in *Xenopus* oocytes and analyzed using two-electrode voltage clamp. The cysteine substitutions had little to no effect on GABA and pentobarbital EC_{50} values. Tethering chemically diverse thiol-reactive methanethiosulfonate reagents onto α_1K219C and α_1K221C affected GABA- and pentobarbital-activated currents differently, suggesting that the pre-M1 structural elements important for GABA and pentobarbital current activation are distinct. Moreover, pentobarbital altered the rates of cysteine modification by methanethiosulfonate reagents differently than GABA. For α_1K221Cβ_2 receptors, pentobarbital decreased the rate of cysteine modification whereas GABA had no effect. For $\alpha_1\beta_2$K215C receptors, pentobarbital had no effect whereas GABA increased the modification rate. The competitive GABA antagonist SR-95531 and a low, non-activating concentration of pentobarbital did not alter their modification rates, suggesting that the GABA- and pentobarbital-mediated changes in rates reflect gating movements. Overall, the data indicate that the pre-M1 region is involved in both GABA- and pentobarbital-mediated gating transitions. Pentobarbital, however, triggers different movements in this region than GABA, suggesting their activation mechanisms differ.

Ligand-gated ion channels (LGICs)[2] are integral membrane proteins that mediate fast synaptic transmission between cells in the brain and at the neuromuscular junction. The type A γ-aminobutyric acid receptor ($GABA_A$R) is the main inhibitory LGIC in the brain and is the target for a wide range of therapeutic agents such as benzodiazepines, barbiturates, and anesthetics. Barbiturates, such as pentobarbital (PB), have three distinct effects on $GABA_A$R activity. At low concentrations, PB modulates GABA-mediated Cl^- current (I_{GABA}). At higher concentrations, PB directly activates the $GABA_A$R in the absence of GABA, and at still higher concentrations, PB blocks channel activity (1). Little is known, however, about the structural rearrangements underlying these functional effects.

Single channel studies from mouse spinal neurons (2–4) and from rat hippocampal neurons (5) have shown that currents evoked by PB are similar in conductance as those evoked by GABA, suggesting that the open state structures stabilized by PB binding are similar to those stabilized by GABA. However, GABA and PB bind to distinct sites on the $GABA_A$R (Fig. 1). The GABA binding site is located at the interfaces of the α_1 and β_2 subunits in the extracellular domain, whereas the PB/general anesthetics binding site(s) are believed to be located ~50 Å below the GABA binding site in a water-accessible pocket located between the four transmembrane helices (M1–4) of the receptor (Fig. 1). Mutational analyses as well as photolabeling studies have identified positions in the $GABA_A$R transmembrane helices that are important for mediating the effects of PB/anesthetics, with a proposed binding pocket involving residues in M1 (α_1M236), M2 (β_2N265), and M3 (β_2M286) (6–8).

The structural machinery associated with coupling agonist binding to channel gating in the Cys-loop family of LGICs likely involves distributed movements of, and interactions between, several discrete domains. Recent evidence suggests that binding of neurotransmitter in the extracellular domain triggers a series of molecular motions (conformational wave) that initiates in the ligand binding pocket, followed by movements in Loop 2, Loop 7 (Cys-loop), the pre-M1 region, the M2-M3 linker, and finally the transmembrane domains to gate the channel (9–11). Because PB- and GABA-activated channel open state structures are alike (3, 12) but PB and GABA bind to different sites, we were interested in determining whether gating motions induced by PB are similar to those induced by GABA.

* This work was supported, in whole or in part, by National Institutes of Health Grant NS34727 from NINDS (to C. C.). This work was also supported by the Diversity Program in Neuroscience of the American Psychological Association (to J. M.). The costs of publication of this article were defrayed in part by the payment of page charges. This article must therefore be hereby marked "*advertisement*" in accordance with 18 U.S.C. Section 1734 solely to indicate this fact.

[1] To whom correspondence should be addressed: University of Wisconsin-Madison, 601 Science Dr., Madison, WI 53711. Tel.: 608-265-5863; E-mail: czajkowski@physiology.wisc.edu.

[2] The abbreviations used are: LGIC, ligand-gated ion channel; $GABA_A$R, γ-aminobutyric acid type A receptor; PB, pentobarbital; MTS, methanethiosulfonate; MTS, MTS-ethyltrimethylammonium; MTSES, MTS-ethylsulfonate.

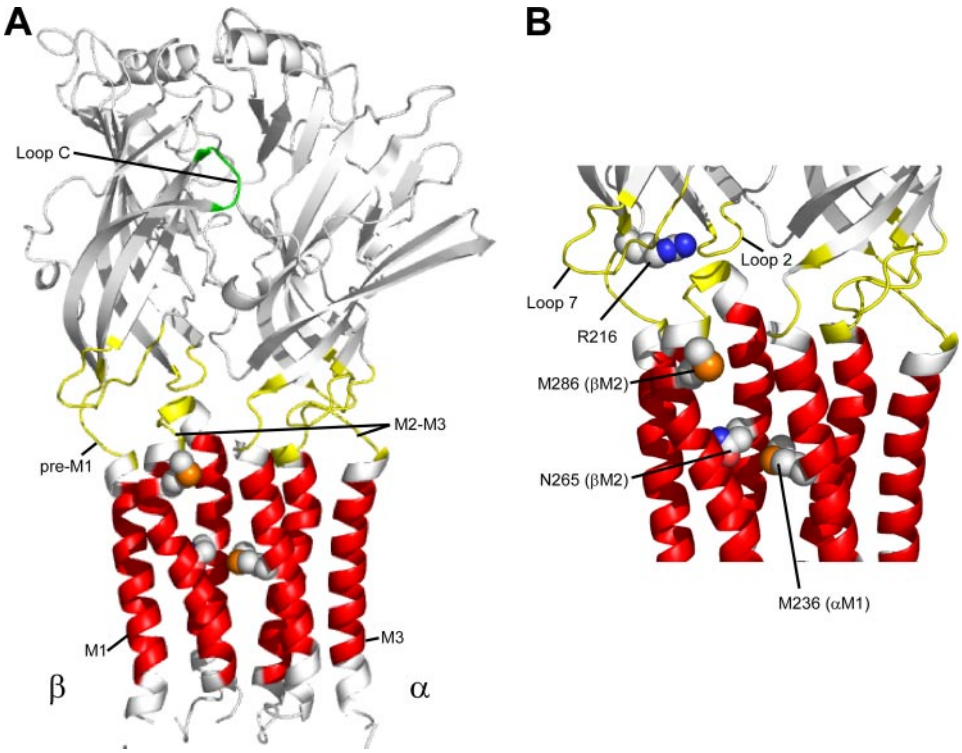

FIGURE 1. **Structural model of the $GABA_AR$ α_1 and β_2 subunits.** *A*, the extracellular binding domain is colored in *white*. Domains believed to contribute to the GABA transduction mechanism (Loop 2, Loop 7, M2-M3 linker, and pre-M1) are highlighted in *yellow*. The Loop C region of the GABA binding site is highlighted in *green*. The transmembrane domains (*M1*, *M2*, and *M3*) are colored in *red*. Residues in the pre-M1 region (Arg-216) as well as residues forming the potential PB/general anesthetic binding site (Asn-265 and Met-286) in the β_2 subunit and (Met-236) in the α_1 subunit are shown in a *space-filled* format. The M4 transmembrane helix has been omitted for illustration purposes. *B*, detailed view of the interface between the ligand binding domain and the transmembrane domain.

We previously demonstrated that the α_1 and β_2 pre-M1 regions of the $GABA_AR$, which connect the extracellular domain of each subunit with the transmembrane domain, undergo structural rearrangements during GABA activation (13). In this study, we measured PB-mediated changes in the accessibility of cysteines engineered into the pre-M1 region to monitor structural movements induced by activating concentrations of PB and compared these changes to those induced by GABA. Our data indicate that the pre-M1 region is part of a common gating pathway used by both ligands. PB, however, triggers different movements in this region than GABA, suggesting that structural transitions evoked and/or stabilized by PB binding/channel activation differ from those triggered by GABA.

EXPERIMENTAL PROCEDURES

Mutagenesis—Rat cDNAs encoding α_1 and β_2 $GABA_AR$ subunits were used for all molecular cloning and functional studies. Cysteine mutants were made as previously described (13).

Expression in Xenopus laevis Oocytes—Oocytes were prepared as previously described (14). Capped cRNAs encoding the α_1, β_2, α_1K219C, α_1K221C, β_2K213C and β_2K215C subunits in the vector pGH19 (15, 16) were transcribed *in vitro* using the mMessage mMachine T7 kit (Ambion, Austin, TX). Single oocytes were injected within 24 h with 27 nl of cRNA (10 ng/μl/subunit) in a ratio 1:1. Oocytes were incubated at 18 °C in ND96 (in mM: 96 NaCl, 2 KCl, 1 $MgCl_2$, 1.8 $CaCl_2$, and 5 HEPES, pH 7.2) supplemented with 100 μg/ml gentamycin and 100 μg/ml bovine serum albumin for 2–7 days before use.

Two-electrode Voltage Clamp—Oocytes were continuously perfused at a rate of ~5 ml/min with ND96 while being held under two-electrode voltage clamp at −80 mV. The bath volume was ~200 μl. Stock solutions of GABA (Sigma-Aldrich) and PB (Research Biochemicals, Natick, MA) were prepared fresh daily in ND96. Borosilicate electrodes (Warner Instruments, Hamden, CT) were filled with 3 M KCl and had resistances between 0.7 and 2 MΩ. Electrophysiological data were acquired with a GeneClamp 500 (Axon Instruments, Foster City, CA) interfaced to a computer with an ITC16 analog-to-digital device (Instrutech, Great Neck, NY) and recorded using Whole Cell Program 3.2.9 (kindly provided by J. Demspter, University of Strathclyde, Glasgow, Scotland).

Concentration Response Analysis—PB concentration responses were measured, and the resulting data were fit to the following equation: $I = I_{max}/(1 + (EC_{50}/[A])^n)$, where I is the peak response to a given concentration of PB, I_{max} is the maximum amplitude of current, EC_{50} is the concentration of PB that evokes half-maximal response, $[A]$ is the agonist concentration, and n is the Hill coefficient. At high PB concentrations, currents were partially blocked during PB application. Thus, peak PB currents were measured immediately after PB wash out, when a prominent tail current appears (21). GraphPad Prism 4 software (San Diego, CA) was utilized for data analysis and fitting.

Modification of Introduced Cysteine Residues by MTS Reagents—Three derivatives of methanethiosulfonate (CH_3SO_2X; MTS) were used to covalently modify the introduced cysteines: MTS-*N*-biotinylaminoethyl (X = SCH_2CH_2NH-biotin; MTSEA-biotin), MTS-ethyltrimethylammonium ($X = SCH_2CH_2N(CH_3)_3^+$; $MTSET^+$), and MTS-ethylsulfonate ($X = SCH_2CH_2\ SO_3^-$; $MTSES^-$) (Biotium, Hayward, CA). $MTSET^+$ is positively charged whereas $MTSES^-$ is negatively charged at neutral pH. Stock solutions (100 mM) were made in DMSO for all MTS reagents, aliquoted into microcentrifuge tubes, and rapidly frozen on ice before storage at −20 °C. For each application of MTS reagent, a new aliquot was thawed, diluted in ND96 to the working concentration, and used immediately to avoid hydrolysis of the MTS compound. The final DMSO concentrations were ≤2%, which had no effect on PB-mediated current responses.

MTS modifications of the engineered cysteines were assayed by measuring changes in PB-evoked current (I_{PB}). The effects of MTSEA-biotin, $MTSET^+$, and $MTSES^-$ were studied using the following protocol: PB (EC_{40-60}) current responses (10 s) were

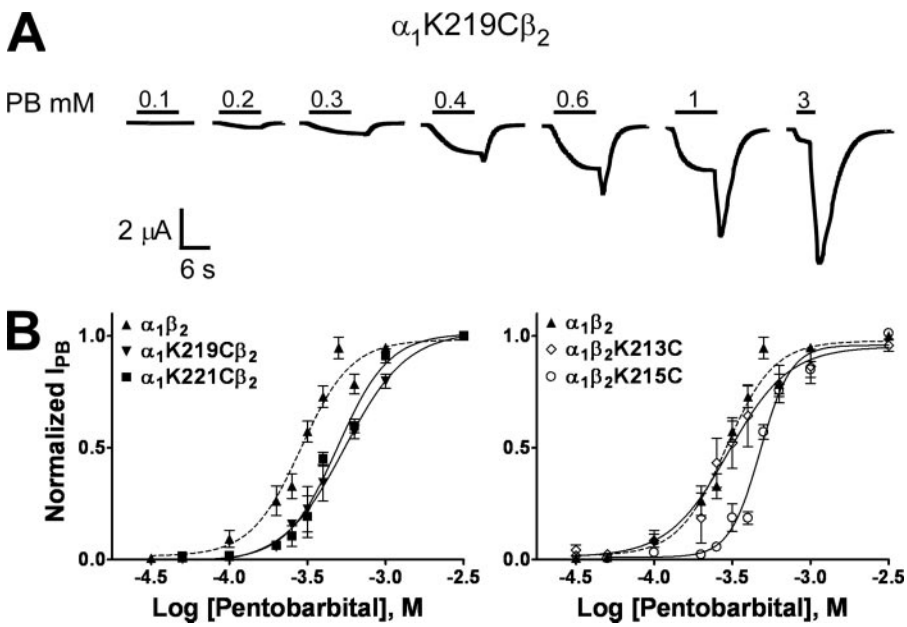

FIGURE 2. **PB concentration response curves of wild-type $\alpha_1\beta_2$ and mutant GABA$_A$R.** *A,* representative current responses from an oocyte expressing α_1K219Cβ_2 receptors elicited by increasing concentrations of PB (mM). *B,* PB concentration response curves from oocytes expressing $\alpha_1\beta_2$ (▲; *dashed line*), α_1K219Cβ_2 (▼), α_1K221Cβ_2 (■), $\alpha_1\beta_2$K213C (◇), and $\alpha_1\beta_2$K215C (○) receptors. Peak PB-activated currents were measured after PB wash out (tail current) and used for concentration response fitting. Data points represent the mean ± S.E. from four to six independent experiments. Data were fit by nonlinear regression analysis as described under "Experimental Procedures." PB EC_{50} and n_H values are reported in Table 1.

measured from oocytes expressing wild-type ($\alpha_1\beta_2$) or mutant receptors and stabilized. Stability was defined as <10% variance of peak current responses to PB on two consecutive applications. After stabilization, the MTS reagent (2 mM) was bath-applied for 2 min, followed by a 5-min wash, and then I_{PB} was measured at the same concentration as before the MTS treatment. The effect of the MTS application was calculated as: $[((I_{after}/I_{initial}) - 1) \times 100]$, where I_{after} is the peak PB current elicited after the MTS application and $I_{initial}$ is the peak current before MTS.

Rate of MTS Modification—The rates at which the various MTS reagents modified the engineered cysteines were determined by measuring the effect of sequential applications of low concentrations of MTS reagents on I_{GABA} as described previously (17). The protocol is described as follows: EC_{40-60} GABA was applied for 10 s every 3–5 min until I_{GABA} stabilized (<3% variance). After a 40-s ND96 wash out, MTS reagents were applied for 5–20 s, and the cell was washed for an additional 2.5–4.5 min. The procedure was repeated until I_{GABA} no longer changed, indicating that the reaction had proceeded to apparent completion. Concentration of MTS reagent and time of application varied as follows: α_1K219C: MTSEA-biotin, 10 μM, 20 s; α_1K221C: MTSEA-biotin, 10 μM, 20 s; β_2K213C: $MTSET^+$, 30 μM, 20 s; β_2K215C: $MTSET^+$, 30 μM, 20 s. The effects of co-applying GABA, SR-95531 (GABA antagonist), or PB (modulator) on reaction rates were assayed by co-applying GABA (EC_{80-90}), 10 μM SR-95531, or PB (50 or 500 μM) with the MTS reagent. For these experiments, I_{GABA} was stabilized as follows: EC_{40-60} GABA was applied for 10 s, washed for 40 s, high concentrations of GABA, SR-95531, or PB were applied for 5–20 s, and the oocyte washed for 2.5–5 min. The procedure was repeated until I_{GABA} from EC_{40-60} GABA was <3% of the previous I_{GABA} peak. This allowed complete wash out of the different drugs and ensured that any alteration in the current amplitudes following MTS treatment in the presence of drug was the result of MTS modification and not a result of inadequate wash out of drug. Concentrations of MTS reagents and times of applications in the presence of GABA (EC_{80-90}) were as follows: α_1K219C: MTSEA-biotin, 30 μM, 20 s; α_1K221C: MTSEA-biotin, 10 μM, 20 s; β_2K213C: $MTSET^+$, 30 or 60 μM, 10 s; β_2K215C: $MTSET^+$, 30 μM, 10 s. In the presence of 500 μM PB: α_1K219C: MTSEA-biotin, 30 μM, 20 s; α_1K221C: MTSEA-biotin, 10 μM, 20 s; β_2K213C: $MTSET^+$, 30 μM, 20 s; β_2K215C: $MTSET^+$, 30 μM, 10 s. In the presence of 50 μM PB: α_1K219C: MTSEA-biotin, 30 μM, 20 s; α_1K221C: MTSEA-biotin, 10 μM, 20 s; β_2K213C: $MTSET^+$, 30 μM, 20 s; β_2K215C: $MTSET^+$, 50 μM, 10 s. In the presence of 10 μM SR-95531: α_1K219C: MTSEA-biotin, 100 μM, 10 s; α_1K221C: MTSEA-biotin, 100 μM, 10 s; β_2K213C: $MTSET^+$, 50 μM, 10 s; β_2K215C: $MTSET^+$, 75 μM, 20 s.

For all rate experiments, the decrease or increase in GABA-induced current was plotted *versus* cumulative time of MTS exposure. Peak current at each time point was normalized to the initial peak current ($t = 0$) and fit to a single exponential function using GraphPad Prism software to obtain a pseudo-first-order rate constant (k_1). The second-order rate constant (k_2) was calculated by dividing k_1 by the concentration of the MTS reagent used (18).

Statistical Analysis—Log (EC_{50}) values, changes in PB EC_{50} after MTS modification, and second-order (k_2) rates were analyzed using a one-way analysis of variance, followed by a post-hoc Dunnett's test to determine the level of significance between wild-type and mutant receptors.

Structural Modeling—A model of the entire $GABA_A$ receptor was built as previously described (13).

RESULTS

Functional Characterization of Pre-M1 Mutant Receptors—We previously showed (13) that cysteine substitutions in the pre-M1 region of the α_1 (K219C, K221C) and β_2 (K213C, K215C) subunits had no effects on GABA EC_{50} ($\alpha_1\beta_2$ receptors, $EC_{50} = 6.9 \pm 0.7$ μM). To determine whether the same cysteine substitutions altered PB activation, we measured PB concentration responses using two-electrode voltage clamp (Fig. 2). Cysteine substitutions of α_1K219, α_1K221, and β_2K215 had little (2-fold) to no effect (β_2K213) on PB EC_{50} values relative to $\alpha_1\beta_2$ receptors ($EC_{50} = 271 \pm 18$ μM; Fig. 2; Table 1). Mutant receptors had Hill coefficients for PB activation that were not significantly different from wild-type $\alpha_1\beta_2$ receptors (Table 1). PB

TABLE 1

PB concentration response data for $\alpha_1\beta_2$ and mutant receptors

Concentration response data for PB activation of wild-type and mutant receptors are tabulated. EC_{50} and Hill coefficient (n_H) values are expressed as mean ± S.E. for n number of independent experiments from at least two batches of oocytes. *, $p < 0.05$, **, $p < 0.01$, significantly different from control.

Receptor	EC_{50}	n_H	n
	μM		
$\alpha_1\beta_2$	271 ± 18	2.7 ± 0.3	6
α_1(K219C)β_2	495 ± 32**	2.4 ± 0.2	4
α_1(K221C)β_2	471 ± 41*	2.8 ± 0.4	5
$\alpha_1\beta_2$(K213C)	224 ± 5.1	2.5 ± 0.4	5
$\alpha_1\beta_2$(K215C)	577 ± 44**	3.8 ± 0.5	4

maximal macroscopic currents elicited from mutant receptors were similar to $\alpha_1\beta_2$ receptors, ranging from 600 nA to 18 μA. The fact that these mutations had little effect on GABA and PB EC_{50} values, Hill coefficients, or surface expression suggests that the side chains of the introduced cysteines are in similar positions as the side chains of the native residues, making the introduced cysteines at positions α_1K219, α_1K221, β_2K213, and β_2K215 ideal candidates to probe the dynamics of the pre-M1 region induced by PB binding/gating.

Effects of Cysteine Modification on PB- and GABA-evoked Currents—We measured current responses elicited with PB EC_{50} (I_{PB}) concentrations before and after MTS reagent application (Fig. 3) to examine how covalently modifying the introduced cysteines would affect PB currents. The MTS reagents used were 1) MTSEA-biotin, which covalently adds a neutral biotinylaminoethyl group (12 Å long); 2) $MTSET^+$, which adds a positively charged ethyl-trimethylammonium group (4.5 Å long); and 3) $MTSES^-$, which adds a negatively charged ethylsulfonate group (4.8 Å long). Application of 2 mM MTSEA-biotin, $MTSET^+$, or $MTSES^-$ for 2 min to wild-type receptors had no effect on I_{PB} (≤5 ± 3% for all reagents), indicating that any effects observed in the mutant receptors are due to modification of the introduced cysteines (Fig. 3*B*). MTSEA-biotin modification of β_2K213C and β_2K215C increased I_{PB} by 86 ± 12 and 31 ± 4% ($n \geq 3$), respectively, and decreased I_{PB} by 72 ± 3% ($n = 6$) in α_1K221C-containing receptors (Fig. 3*B*). Similar functional effects on GABA EC_{50} current responses (I_{GABA}) were observed after MTSEA-biotin modification of β_2K213C, β_2K215C, and α_1K221C (Fig. 3*B* and Ref. 13). In contrast, MTSEA-biotin modification of α_1K219C did not affect I_{PB} whereas I_{GABA} was increased by 34 ± 2% (Fig. 3*B*). This indicates that MTSEA-biotin covalently modified α_1K219C but modification had no functional effect (*i.e.* a "silent" reaction) on PB-induced currents.

Derivatization of β_2K213C and β_2K215C with $MTSES^-$ increased I_{PB} by 50 ± 3 and 53 ± 16%, respectively, while $MTSET^+$ increased I_{PB} 133 ± 2 and 56 ± 5%, respectively ($n \geq 3$) (Fig. 3*B*). Similar functional effects on I_{GABA} were observed after derivatization of β_2K213C and β_2K215C with $MTSES^-$ or $MTSET^+$ (13) (Fig. 3*B*). As we previously reported, modification of α_1K219Cβ_2 and α_1K221Cβ_2 by $MTSES^-$ and $MTSET^+$ differentially affected I_{GABA} (Fig. 3*B*). Tethering a negative charge ($MTSES^-$) onto α_1K221C enhanced I_{GABA} (98 ± 14%; $n = 4$), whereas treatment with the positively charged $MTSET^+$ had no functional effect on I_{GABA} (Fig. 3*B*). In contrast, tethering a positive charge ($MTSET^+$) onto

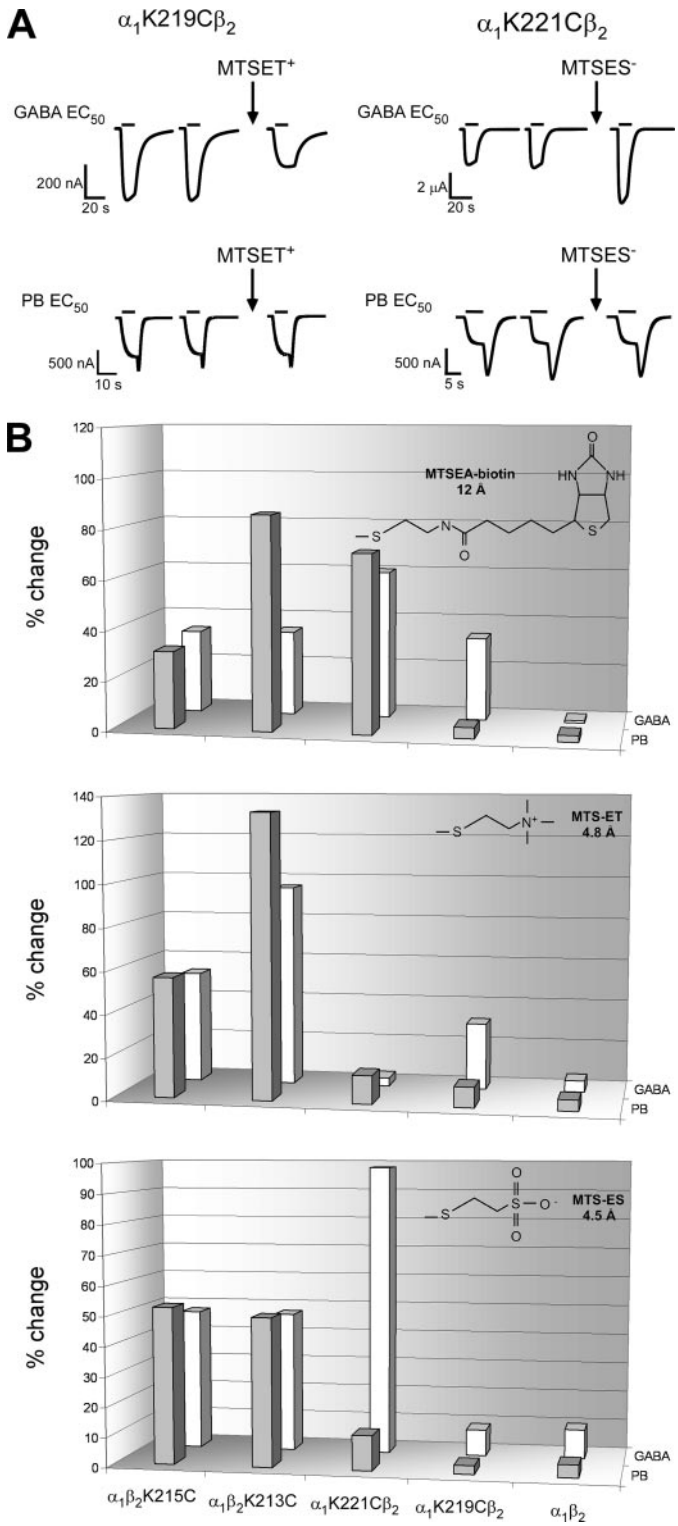

FIGURE 3. **Effects of MTS reagents on $\alpha_1\beta_2$ and mutant $GABA_AR$.** *A*, representative current traces elicited by GABA (*top traces*) or PB (*bottom traces*) of EC_{50} concentrations from oocytes expressing α_1K219Cβ_2 and α_1K221Cβ_2 receptors before and after treatment with $MTSET^+$ and $MTSES^-$ (2 min, 2 mM). $MTSET^+$ and $MTSES^-$ treatment altered the GABA current responses but had no effect on PB current responses. *B*, summary of the effects of a 2-min application of 2 mM MTSEA-biotin (*top*), $MTSET^+$ (*middle*), or $MTSES^-$ (*bottom*) on GABA (EC_{50}) -activated currents (I_{GABA}) (previously reported in Ref. 13) and PB (EC_{50}) -activated currents (I_{PB}) from $\alpha_1\beta_2$ and mutant receptors. The absolute percent change in I_{PB} and I_{GABA} after MTS treatment is defined as: $[(I_{after}/I_{initial}) - 1) \times 100]$. *Bars* represent the mean from at least three independent experiments. Values >20% are significantly different from $\alpha_1\beta_2$ values ($p < 0.01$).

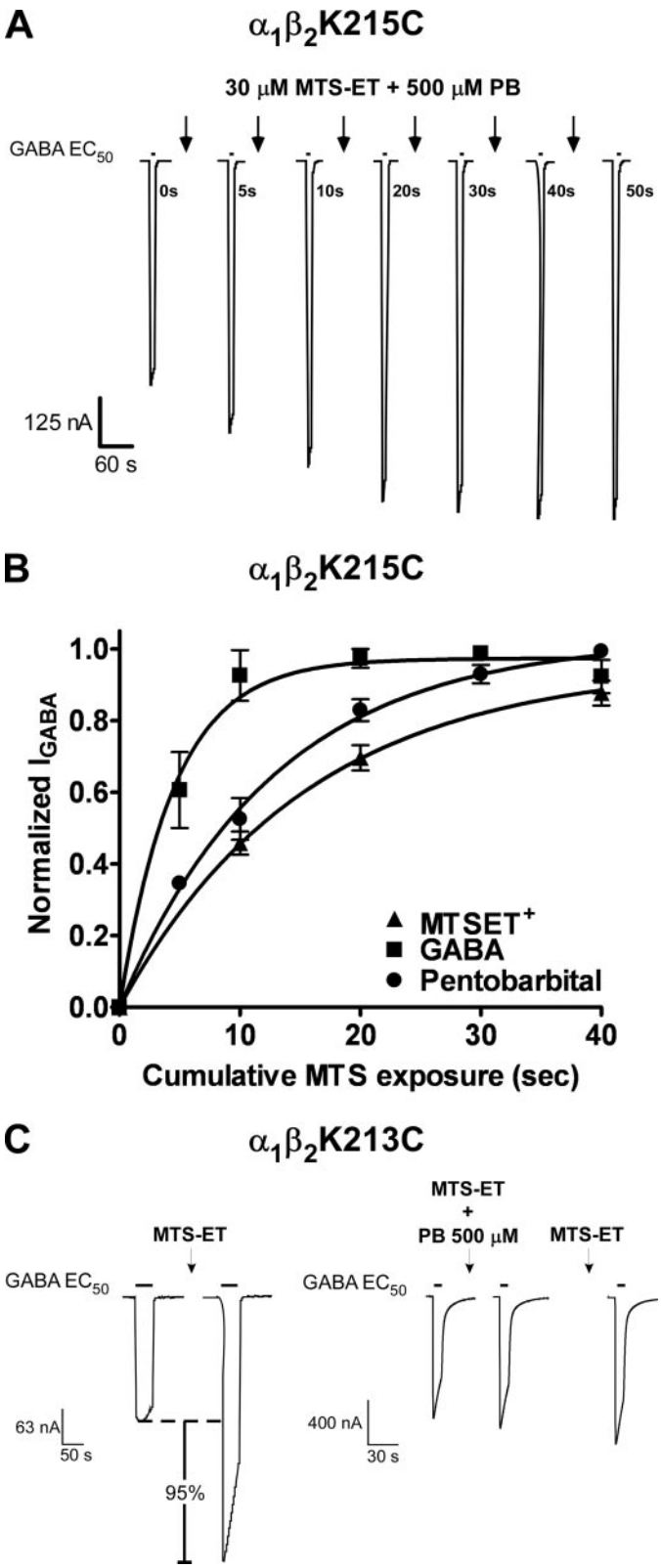

FIGURE 4. **Rates of MTSET$^+$ modification of $\alpha_1\beta_2$K215C receptors in the presence and absence of GABA or PB.** *A,* representative GABA current traces recorded while applying MTSET$^+$ (30 μM) in the presence of PB (500 μM). GABA EC_{40-60} current responses were recorded before and after successive application (10 s) of 30 μM MTSET$^+$ co-applied with PB (*arrows*). *B,* normalized GABA current responses were plotted *versus* cumulative time of MTSET$^+$ (▲), MTSET$^+$ co-applied with EC_{80-90} GABA (■), and MTSET$^+$ co-applied with 500 μM PB (●) and fit with single exponential functions. Data were normalized to the maximal amount of potentiation of I_{GABA} for each experiment and represent mean ± S.E. from at least three independent experiments. *C,* representative GABA-mediated current traces from oocytes expressing $\alpha_1\beta_2$K213C receptors. Currents elicited by an EC_{50} concentration of GABA were recorded before and after MTSET$^+$ (2 mM, 2 min) in the absence or presence of 500 μM PB. MTSET$^+$ treatment alone potentiated the subsequent current response (95%), but when MTSET$^+$ was co-applied with 500 μM PB the treatment had no functional effect. On the subsequent GABA current and following wash out, MTSET treatment alone no longer resulted in a significant potentiation of current.

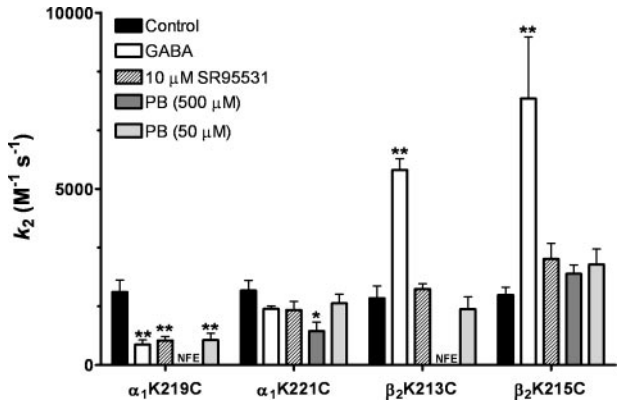

FIGURE 5. **Summary of effects of GABA, PB, and SR-95531 on MTS second-order rate constants.** Second-order rate constants (k_2) for MTS modification of cysteine mutants in the absence and presence of EC_{80-90} GABA, 500 μM PB, 50 μM PB, or 10 μM SR-95531. k_2 values are reported in Table 2. Data are the mean ± S.E. from at least three independent experiments. * and ** indicate values significantly different from control at $p < 0.05$ and $p < 0.001$, respectively. NFE (no functional effect) MTS reagent reacts with the cysteine mutant in the presence of PB but has no functional effect on subsequent GABA responses.

α_1K219C decreased I_{GABA} (31 ± 7%; $n = 3$), whereas modification with MTSES$^-$ had no effect. These results are likely due to differences in the local electrostatic environments near α_1K219C and α_1K221C rather than steric effects because MTSET$^-$ and MTSES$^+$ are similar in size (Fig. 3*B*, *insets*) and have a common reaction mechanism. Surprisingly, modification of α_1K219Cβ_2 and α_1K221Cβ_2 by MTSES$^-$ or MTSET$^+$ had no functional effects on I_{PB} (Fig. 3*A*), indicating that introducing a positive or negative charge at these positions has different effects on PB and GABA current responses, suggesting that the physicochemical structural elements in the pre-M1 region important for GABA and PB current activation are distinct.

Effect of PB on MTS Reaction Rates—To determine whether PB binding/gating induces different structural rearrangements in the pre-M1 regions than GABA, we measured the rates of MTS modification of α_1K219C, α_1K221C, β_2K213C, and β_2K215C in the presence of a directly activating concentration of PB (500 μM) and compared these to rates measured in the presence of GABA (Figs. 4 and 5). The rate of modification of a cysteine by a MTS reagent mainly depends on the ionization of the thiol group and the access pathway of the reagent. Thus, changes in rates measured in the presence of PB or GABA provide a measure of structural changes in the receptor that are triggered by their binding. PB had no effect on the MTSET$^+$ rate of modification of $\alpha_1\beta_2$K215C whereas GABA increased the rate by 4-fold. For α_1K221Cβ_2 receptors, PB decreased the MTSEA-biotin rate by 2-fold whereas GABA had no significant effect. For $\alpha_1\beta_2$K213C receptors and α_1K219Cβ_2 receptors, GABA increased and decreased their rates of modification by 3-

TABLE 2

Second-order rate constants (k_2) for reaction of MTS reagents with mutant receptors in the absence (*Control*) and presence of GABA, PB, and SR-95531

NFE, no functional effect; MTS reagents react but have no functional effect on subsequent GABA responses. *, ** indicate values significantly different from control, with $p < 0.05$ and $p < 0.001$, respectively. Values are the mean ± S.E.

Receptor	Control[a]		GABA[a] EC_{80-90}		SR-95531		Pentobarbital		Pentobarbital	
	k_2 $M^{-1}s^{-1}$	*n*	k_2 $M^{-1}s^{-1}$	*n*	k_2 $M^{-1}s^{-1}$	*n*	k_2 $M^{-1}s^{-1}$	*n*	k_2 $M^{-1}s^{-1}$	*n*
					10 μM		*500 μM*		*50 μM*	
α_1K219Cβ_2[b]	2070 ± 300	4	580 ± 130**	3	700 ± 110**	4	NFE	3	710 ± 190	4
α_1K221Cβ_2[b]	2110 ± 290	6	1600 ± 80	4	1570 ± 250	4	970 ± 250*	4	1750 ± 260	3
$\alpha_1\beta_2$K213C[c]	1900 ± 340	5	5540 ± 320**	7	1610 ± 200	4	NFE	3	1590 ± 340	3
$\alpha_1\beta_2$K215C[c]	1990 ± 220	6	7560 ± 1750**	3	3050 ± 510	3	2590 ± 250	3	2850 ± 440	4

[a] Reported in Ref. 13.
[b] MTSEA-biotin reaction rates are reported.
[c] $MTSET^+$ reaction rates are reported.

and 4-fold, respectively. In contrast, when PB was present during the MTS reaction, the MTS treatment no longer altered subsequent GABA current responses for $\alpha_1\beta_2$K213C and α_1K219Cβ_2 receptors (Fig. 4*C*). A subsequent application of MTS reagent in the absence of PB had little effect on GABA current, indicating that the thiol was modified in the presence of PB but modification now resulted in no detectable effect on I_{GABA}. Although the mechanism underlying this loss of functional effect is unknown, one can conclude that cysteine modification in the presence of 500 μM PB is different from modification in the presence of GABA. A low concentration of PB that does not activate the receptor but potentiates GABA responses (50 μM) decreased the rate of modification of α_1K219C by ~3-fold and had no effect on the rates of modification of α_1K221C, β_2K213C, and β_2K215C (Fig. 4, Table 2), indicating that the effects of PB (500 μM) on α_1K221Cβ_2 and $\alpha_1\beta_2$K213C receptors likely reflect gating-associated motions. Overall, these data indicate that GABA and PB induce different structural rearrangements in the pre-M1 regions of the α_1 and β_2 subunits.

Effect of SR-95531 on MTS Reaction Rates—To explore whether the structural rearrangements in the pre-M1 regions induced by GABA reflect conformational movements associated with gating, we measured the rates of MTS modification of α_1K219C, α_1K221C, β_2K213C, and β_2K215C in the presence of the GABA binding site competitive antagonist SR-95531 (10 μM) (Fig. 5). Because GABA and SR-95531 bind to the same site, but GABA promotes channel opening/desensitization whereas SR-99531 does not, co-application of SR-95531 and MTS should capture motions associated with stabilization of a closed state whereas co-application of GABA and MTS should capture motions associated with open/desensitized states (*i.e.* gating). SR-95531 had no significant effect on the rate of modification of α_1K221Cβ_2, $\alpha_1\beta_2$K213C, and $\alpha_1\beta_2$K215C receptors compared with control (Fig. 5 and Table 2), suggesting that occupancy of the GABA binding site alone does not induce structural rearrangements in or near these positions. SR-95531 slowed the MTSEA-biotin rate of modification of α_1K219Cβ_2 receptors 3-fold (Fig. 5 and Table 2), indicating that binding of a competitive antagonist can induce structural rearrangements in the pre-M1 region of the α_1 subunit.

DISCUSSION

The Monod-Wyman-Changeux allosteric theory has been used with great success to model LGIC gating behavior (19). In this theory, channel gating is accomplished by a concerted quaternary movement of all the subunits switching from an inactive to an active conformation. GABA and PB activation both evoke the same single channel conductances (3) despite binding to different parts of the receptor (20). Thus, a key question is whether binding of an allosteric modulator such as PB triggers similar allosteric gating transitions as GABA.

For Cys-loop LGICs, it has been suggested that the pre-M1 region acts as a central hub that couples neurotransmitter-induced motions in the ligand binding site to movements in Loop 2 and the M2-M3 linker, which then ultimately triggers movements in the M2 channel region that opens the channel (Fig. 1) (10, 13). A key element in the transduction pathway coupling neurotransmitter binding to gating of the channel is believed to be a salt bridge between two highly conserved residues present in all Cys-loop LGIC subunits: an arginine in the pre-M1 region with a glutamic acid in Loop 2 (Fig. 1) (10). Previously, we showed that cysteine substitution of this highly conserved arginine (Arg-216) in the β_2 pre-M1 region of the $GABA_AR$ abolished channel gating by GABA without altering binding of the GABA agonist [^{3}H]muscimol (13), suggesting that this residue plays a key role in allosterically coupling GABA binding to gating. Interestingly, the β_2R216C mutation also abolished channel gating by PB, suggesting that this residue and the pre-M1 region may also play a role in PB activation (13).

Here, we provide evidence that the α_1 and β_2 pre-M1 regions move in response to PB activation of the $GABA_AR$ and that PB triggers different movements in this region than GABA. Cysteine substitutions of the conserved pre-M1 lysine residues had little to no effect on PB EC_{50} (Fig. 2 and Table 1); thus, the positions occupied by the cysteine side chains in the mutant receptors are likely similar to the native lysine positions. The rates of modification of α_1K221Cβ_2, α_1K219Cβ_2, $\alpha_1\beta_2$K213C, and $\alpha_1\beta_2$K215C receptors differ depending upon whether GABA or PB is present. For α_1K221Cβ_2 receptors, only 500 μM PB caused a significant change in the rate of MTS modification whereas for $\alpha_1\beta_2$K215C receptors only GABA caused a change (Fig. 5, Table 2). For α_1K219Cβ_2 and $\alpha_1\beta_2$K213C receptors, GABA altered their rates of modification, whereas in the presence of PB the mutant receptors were modified but MTS modification no longer altered subsequent GABA-induced current (Fig. 5, Table 2), demonstrating that PB stabilizes the receptor in a different conformation(s) than GABA. Moreover, structur-

ally perturbing the pre-M1 regions by tethering chemically diverse thiol-reactive groups onto these mutant cysteines had different effects on PB and GABA current responses (Figs. 2 and 3). Based on these data, we infer that the structural transitions evoked and/or stabilized by PB channel activation differ from those triggered by GABA in this region of the receptor.

Alternatively, one could argue that some of the differences measured in the effects of modifying these cysteines on GABA and PB current responses result from the pre-M1 residues being located near the PB binding site pocket. Several lines of evidence indicate that α_1K219, α_1K221, β_2K213, and β_2K215 do not form part of the PB binding site. First, mutations of these residues to cysteine had little to no effect on PB EC_{50}. If these residues directly formed part of the PB binding site, one would expect bigger shifts in PB EC_{50}, especially because of the non-conservative cysteine for lysine substitution. Second, modification of β_2K213C and β_2K215C with a variety of MTS reagents all increased PB-induced current and modification of α_1K219C had no effects on PB-induced currents. If these residues were lining the PB binding site, one would expect that tethering bulky/charged groups at these positions would sterically inhibit the ability of PB to bind and would decrease PB-mediated current. Although modification of α_1K221C with MTSEA-biotin caused a decrease in PB-mediated current, modification with MTSET and MTSES had no effect on PB-mediated currents, again suggesting that this residue is not part of the PB binding site. Third, PB caused an increase in the rate of MTS modification of β_2K215C. If β_2K215C were part of the PB binding site, one would expect that PB would decrease the rate of modification. Moreover, based on our homology model of the $GABA_AR$ and given the size of PB (~7 Å), it seems unlikely that α_1 and β_2 pre-M1 region residues are forming part of the general anesthetic binding site. Residues in the α_1 and β_2 pre-M1 regions are separated by 20 Å or more from the residues that have been previously identified as forming the potential PB/general anesthetic binding site (Fig. 1) (8, 21–24). Mutations in M2 (Asn-265) and M3 (Met-286) in the β subunit eliminate PB activation of the receptor (8, 25) and the actions of the related general anesthetics etomidate and propofol (26–28). More recently, α_1M236 (in M1) and βM286 (in M3) have been directly identified as being part of a general anesthetic binding site by photolabeling with an etomidate analog (6). Propofol blocks covalent modification of βM286C by sulfhydryl-specific reagents, indicating that this residue forms part of a general anesthetic binding site (29). Furthermore, a knock-in mouse for βN265M removes the immobilizing and hypnotic actions of PB as well as the actions of etomidate and propofol (30). Taken together, the data indicate that general anesthetics, including PB, likely share a similar binding site, which is located in a water-filled pocket ~50 Å below the GABA binding site between M1, M2, and M3.

In the presence of GABA, the receptor undergoes transitions between an ensemble of open and desensitized states (31, 32). If PB were stabilizing similar states as GABA, one might expect similar changes in the rate of modification in the presence of PB and GABA. Because this was not the case, we infer that PB binding/gating induces structural rearrangements near the pre-M1 region that are structurally distinct from movements induced by GABA. Interestingly, a recent report using disulfide-trapping experiments demonstrated that GABA and PB induce a similar open state structure at the 6′-position in M2 (12). This is consistent with functional studies that have shown similar single-channel conductances (2–4) regardless of whether $GABA_AR$ channels are opened by GABA or by PB. We speculate that the unique movements induced by PB and GABA in the pre-M1 regions are the result of their binding to different sites and triggering different activation pathways that lead to their functional effects.

We envision that PB binding between transmembrane helices initiates a conformational change in the M2-M3 linker that propagates to the pre-M1 region via Loop 2 (Fig. 1). Mutational studies have implicated the α_1 and β_2 M2-M3 linker as involved in PB activation (21, 33). The movements in the pre-M1 region triggered by PB are then likely to be transmitted to various regions of the $GABA_AR$ extracellular ligand binding domain as well as channel membrane domain. The pre-M1 region may be the conduit by which the actions of PB are propagated to the GABA binding site. Binding studies have shown that PB enhances GABA apparent affinity (34), suggesting that the structure of the GABA binding site changes in the presence of PB. Moreover, we have identified 13 positions in the GABA binding site interface that change accessibility during pentobarbital binding/gating (β_2T160C, β_2D163C, β_2G203C, β_2S204C, β_2R207C, β_2S209C, β_2D62C, α_1S68C, α_1E122C, α_1R131C, α_1V180C, α_1A181C, and α_1R186C) (17, 35–38), indicating that the extracellular domain undergoes conformational rearrangements during PB binding/gating.

In summary, we have shown that the α_1 and β_2 pre-M1 regions of the $GABA_ARs$ are structural elements involved in both GABA- and PB-mediated channel activation. PB binding, however, induces different structural movements in this region than when the receptor binds GABA, suggesting that PB stabilizes a different state or ensembles of states than GABA. These differences reveal distinct molecular mechanisms of action of these two ligands.

Acknowledgment—We thank Dr. Ken Satyshur for assistance in construction of the structural model.

REFERENCES

1. Belelli, D., Pistis, M., Peters, J. A., and Lambert, J. J. (1999) *Trends Pharmacol. Sci.* **20,** 496–502
2. Mathers, D. A., and Barker, J. L. (1980) *Science* **209,** 507–509
3. Jackson, M. B., Lecar, H., Mathers, D. A., and Barker, J. L. (1982) *J. Neurosci.* **2,** 889–894
4. MacDonald, R. L., Rogers, C. J., and Twyman, R. E. (1989) *J. Physiol.* **417,** 483–500
5. Rho, J. M., Donevan, S. D., and Rogawski, M. A. (1996) *J. Physiol.* **497,** Pt. 2, 509–522
6. Li, G. D., Chiara, D. C., Sawyer, G. W., Husain, S. S., Olsen, R. W., and Cohen, J. B. (2006) *J. Neurosci.* **26,** 11599–11605
7. Pistis, M., Belelli, D., McGurk, K., Peters, J. A., and Lambert, J. J. (1999) *J. Physiol.* **515,** Pt. 1, 3–18
8. Amin, J. (1999) *Mol. Pharmacol.* **55,** 411–423
9. Grosman, C., Zhou, M., and Auerbach, A. (2000) *Nature* **403,** 773–776
10. Lee, W. Y., and Sine, S. M. (2005) *Nature* **438,** 243–247
11. Chakrapani, S., Bailey, T. D., and Auerbach, A. (2004) *J. Gen. Physiol.* **123,** 341–356
12. Rosen, A., Bali, M., Horenstein, J., and Akabas, M. H. (2007) *Biophys. J.* **92,**

3130–3139
13. Mercado, J., and Czajkowski, C. (2006) *J. Neurosci.* **26,** 2031–2040
14. Boileau, A. J., Kucken, A. M., Evers, A. R., and Czajkowski, C. (1998) *Mol. Pharmacol.* **53,** 295–303
15. Liman, E. R., Tytgat, J., and Hess, P. (1992) *Neuron* **9,** 861–871
16. Robertson, G. A., Warmke, J. M., and Ganetzky, B. (1996) *Neuropharmacology* **35,** 841–850
17. Holden, J. H., and Czajkowski, C. (2002) *J. Biol. Chem.* **277,** 18785–18792
18. Pascual, J. M., and Karlin, A. (1998) *J. Gen. Physiol.* **111,** 717–739
19. Monod, J., Wyman, J., and Changeux, J. P. (1965) *J. Mol. Biol.* **12,** 88–118
20. Amin, J., and Weiss, D. S. (1993) *Nature* **366,** 565–569
21. Serafini, R., Bracamontes, J., and Steinbach, J. H. (2000) *J. Physiol.* **524,** Pt. 3, 649–676
22. Mihic, S. J., Ye, Q., Wick, M. J., Koltchine, V. V., Krasowski, M. D., Finn, S. E., Mascia, M. P., Valenzuela, C. F., Hanson, K. K., Greenblatt, E. P., Harris, R. A., and Harrison, N. L. (1997) *Nature* **389,** 385–389
23. Mihic, S. J., and Harris, R. A. (1996) *J. Pharmacol. Exp. Ther.* **277,** 411–416
24. Harrison, N. L., Kugler, J. L., Jones, M. V., Greenblatt, E. P., and Pritchett, D. B. (1993) *Mol. Pharmacol.* **44,** 628–632
25. Pistis, M., Belelli, D., McGurk, K., Peters, J. A., and Lambert, J. J. (1999) *J. Physiol.* **515,** 3–18
26. Belelli, D., Lambert, J. J., Peters, J. A., Wafford, K., and Whiting, P. J. (1997) *Proc. Natl. Acad. Sci. U. S. A.* **94,** 11031–11036
27. Siegwart, R., Jurd, R., and Rudolph, U. (2002) *J. Neurochem.* **80,** 140–148
28. Siegwart, R., Krahenbuhl, K., Lambert, S., and Rudolph, U. (2003) *BMC Pharmacol.* **3,** 13, 1–9
29. Bali, M., and Akabas, M. H. (2004) *Mol. Pharmacol.* **65,** 68–76
30. Zeller, A., Arras, M., Jurd, R., and Rudolph, U. (2007) *BMC Pharmacol.* **7,** 2, 1–12
31. Macdonald, R. L., and Twyman, R. E. (1992) in *Ion Channels* (Narahashi, T., ed), pp. 315–343, Plenum Press, New York
32. Lema, G. M., and Auerbach, A. (2006) *J. Physiol.* **572,** 183–200
33. Sigel, E., Buhr, A., and Baur, R. (1999) *J. Neurochem.* **73,** 1758–1764
34. Olsen, R. W. (1982) *Annu. Rev. Pharmacol. Toxicol.* **22,** 245–277
35. Wagner, D. A., and Czajkowski, C. (2001) *J. Neurosci.* **21,** 67–74
36. Newell, J. G., and Czajkowski, C. (2003) *J. Biol. Chem.* **278,** 13166–13172
37. Newell, J. G., McDevitt, R. A., and Czajkowski, C. (2004) *J. Neurosci.* **24,** 11226–11235
38. Kloda, J. H., and Czajkowski, C. (2007) *Mol. Pharmacol.* **71,** 483–493